Supporting Information

A Neutral Auxiliary Ligand Enhanced Dysprosium(III) single molecule magnet

Xiao-Xiang Chen,[a] Fang Ma,[b] Mei-Xing Xu,[a] Jin-Cheng Bi,[a] Hao-Ling Sun,[*b] Bing-Wu Wang, [*a] and Song Gao [*a]

[a] *Beijing National Laboratory of Molecular Science, College of Chemistry and Molecular Engineering, State Key Laboratory of Rare Earth Materials Chemistry and Applications, Peking University, Beijing, 100871, P. R. China. E-mail: wangbw@pku.edu.cn; gaosong@pku.edu.cn;*

[b] *Department of Chemistry and Beijing Key Laboratory of Energy Conversion and Storage Materials, Beijing Normal University, Beijing 100875, P. R. China. E-mail: haolingsun@bnu.edu.cn.*

1. Experimental section

1.1 General methods.

All manipulations were carried out by using standard Schlenk technique or in N_2 filled glovebox. All chemical reagents were purchased from Sigma-Aldrich, J&K and used without further purification. THF, hexane and toluene were dried by solvent purification system (MB-SPS-800). Elemental analysis was performed on an Elementar Vario MICRO CUBE (Germany) analyzer. Bis(2-(2,5-dimethyl-1H-pyrrol-1-yl)ethyl)amine (**HL**) and $Dy[(Me_3Si)_2N]_3$were prepared according to the literature methods.[1]

1.2 Synthesis of $DyL_2[N(SiMe_3)_2]$ (L=bis(2-(2,5-dimethyl-1H-pyrrol-1-yl)ethyl)amine)

$Dy[(Me_3Si)_2N]_3$ (0.4mmol, 257.5mg) was added into 100mL Schlenk flask with 20mL toluene. To this solution, 20mL toluene solution containing **HL** (0.8mmol, 207.5mg) was added dropwise with stirring at room temperature. After it was stirred for 30 minutes, the reaction was then warm to 80 ℃ and stirred for 12h. Toluene was removed under vacuum to give a light yellow powder. Recrystallization it from hexane gave $DyL_2[N(SiMe_3)_2]$(**1**) as light yellow crystals. Yield: 129.5 mg (39%). Elemental analysis ($C_{38}H_{66}DyN_7Si_2$): Cal. C 54.36%, H 7.92%, N 11.68%. Found C 54.20%, H 8.05%, N 11.79%.

1.3 X-ray crystallography.

The Single-crystal X-ray diffraction data were collected on an Agilent Technology Super Nova Dual Atlas CCD diffractometer, using an monochromator source Mo K_α radiation (λ = 0.71073Å) at 180 K. The data processing was accomplished with the *CrysAlisPro* program. The structures were solved by direct methods and refined on F^2 anisotropically for all the non-hydrogen atoms by the full-matrix least-squares method using *SHELXL* 97 program.[2]

1.4 Magnetic measurements.

Magnetic measurements were performed on Quantum Design MPMS3 magnetometer with crushed polycrystalline sample. The sample was tightly packed and sealed with parafilm then into a gelatin capsule. Diamagnetic corrections of sample were preformed using Pascal constants. Capsule and parafilm background correction were considered.

1.5 *Ab initio* Calculation

The *ab initio* calculations were performed with the CASSCF/RASSI/SINGLE_ANISO type using MOLCAS 8.0 package on the crystal structure without optimization (**Figure S9**).[3] The basis sets for all atoms are atomic natural orbitals from the MOLCAS ANO-RCC library: ANO-RCC-VTZP for Dy(III) ions; ANO-RCC-VTZP for coordinated N; ANO-RCC-VDZ for other atoms. The active space contains nine electrons in seven 4*f* orbitals. In RASSI, 21 spin sextets, 128 spin quartets, 130 spin doublets were mixes by spin-orbit coupling. SINGLE_ANISO module was used to calculate the magnetic properties such as g-tensor, main magnetic axes, magnetic susceptibility and crystal field parameters. The calculation on a reduced structure by remove the coordinated pyrrole ring (**Figure S10**) were performed. All calculation details are the same as full molecule structure.

1.6 Angular-dependent magnetometric study

Taking advantage of the collinearity of the molecular and crystal physical principal axes in this of sample, we were able to investigate the magnetic principal axis. Angular-dependent magnetometric study on single crystal was carried on the MPMSXL5 SQUID magnetometer equipped with a horizontal rotator. We mounted a single crystal of 0.72 mg with the (-100) face glued on an L-shaped Cu/Be support in order to perform a rotation around three orthogonal axes of the support easily. The experimental Cartesian coordiantes XYZ was defined as below. Three series rotation data were collected from 3 K to 7.5 K under 1000 Oe, after then corrected for the diamagnetic contribution from the support and grease. The detailed experimental procedure can be found in the literature.

2. Results and discussion

Table S1. Crystal data and structure refinement for **1**.

Empirical formula	$C_{38}H_{66}DyN_7Si_2$
Formula weight	839.65
Temperature/K	180.00(10)
Crystal system	triclinic
Space group	P-1
a/Å	10.7692(3)
b/Å	10.8103(3)
c/Å	19.6786(5)
α/°	88.619(2)
β/°	80.960(2)
γ/°	69.139(2)
Volume/Å^3	2112.92(10)
Z	2
F(000)	874.0
Goodness-of-fit on F^2	1.070
Final R indexes [I>=2σ (I)]	R1 = 0.0180, wR2 = 0.0446
Final R indexes [all data]	R1 = 0.0195, wR2 = 0.0451

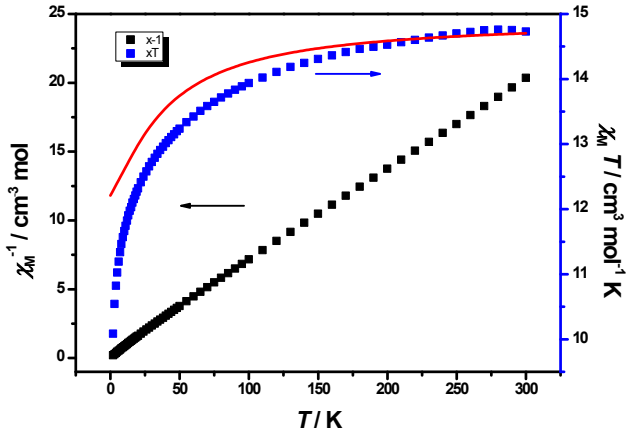

Figure S1. Temperature dependence of dc susceptibility for **1**. The solid squares are experiment data. The red solid line is *ab initio* calculations simulation results with a scaled up by 6% to match the experimental room temperature $\chi_M T$ value.

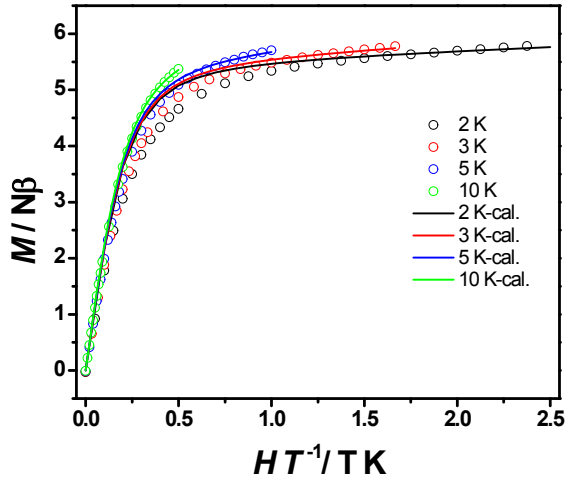

Figure S2. Field dependent magnetization curve for **1**. The circles are experiment data at 2 K(black), 3 K(red), 5 K(blue), 10 K(green). The solid lines are *ab initio* calculations results with a scaled up 6% to match experiment.

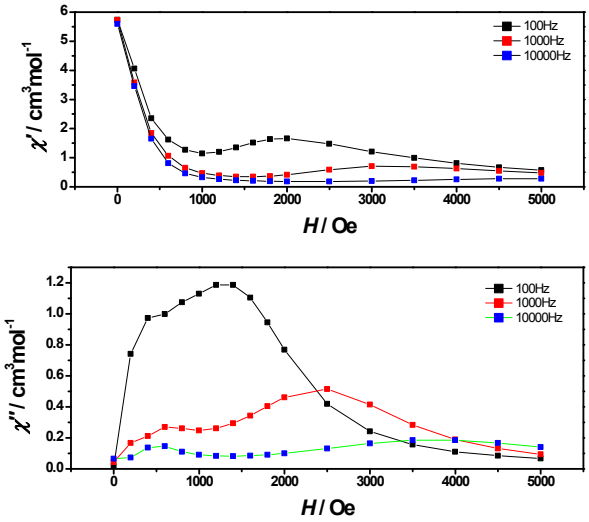

Figure S3. Scan field ac susceptibilities measurement with a 3 Oe ac magnetic field at 2 K and 100 Hz, 1000 Hz, 10000 Hz.

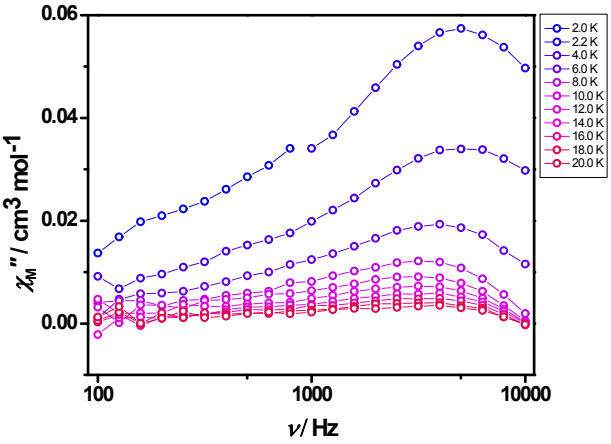

Figure S4. Frequency dependence of out-of-phase magnetic susceptibility for **1** under 0 Oe dc field from 2.0 K to 20.0 K

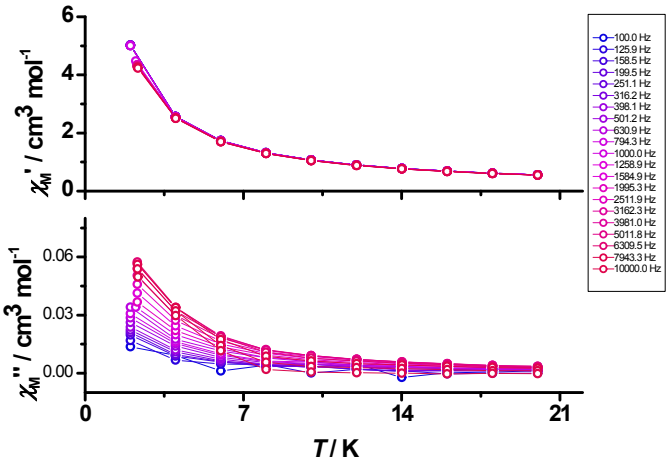

Figure S5. Temperature dependence of in-phase and out-of-phase magnetic susceptibility for **1** under 0 Oe dc field from 2.0 K to 20.0 K.

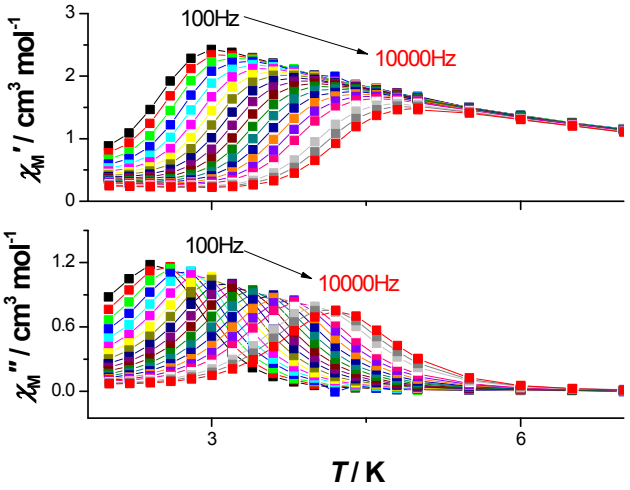

Figure S6. Temperature dependence of in-phase and out-of-phase magnetic susceptibility for 1 under 1000 Oe dc field from 2.0 K to 7.0 K.

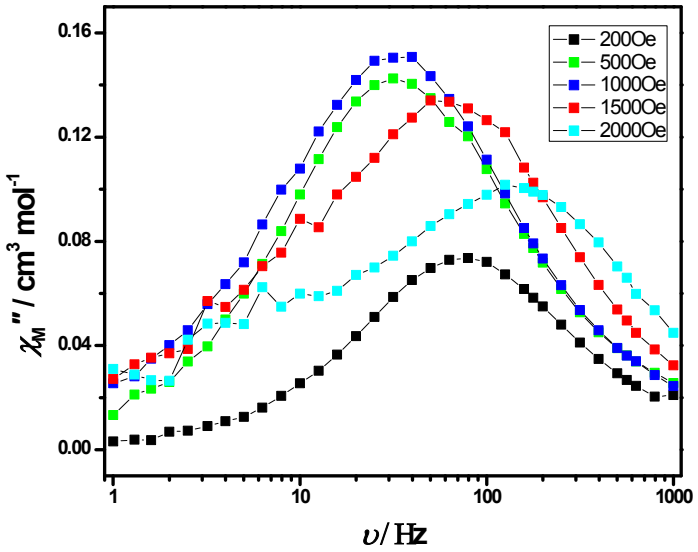

Figure S7. Frequency dependence of the out-of-phase ac magnetic susceptibility for **1** at 2 K under different dc field.

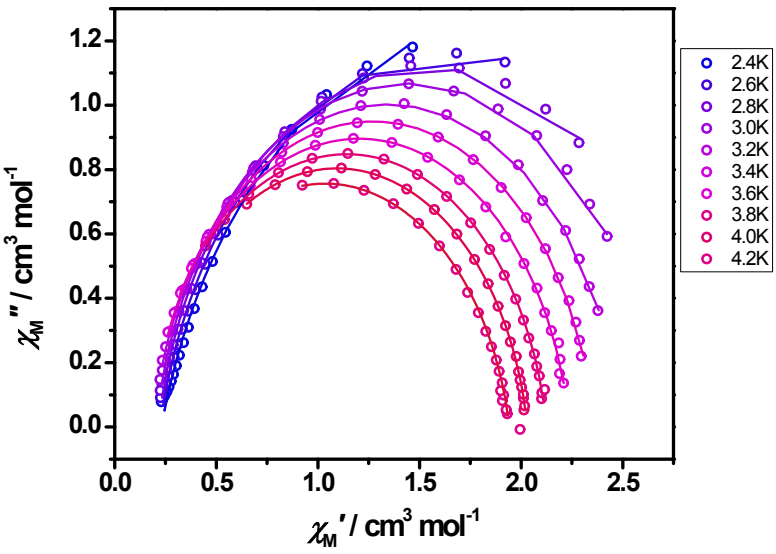

Figure S8. Cole-Cole fitting from 2.4 K to 4.2 K under 1000 Oe static field of **1**.

The in-phase (χ_M') and out-phase (χ_M'') data from 2.4 K to 4.2 K under 1000 Oe static field were analyzed with the one-component Debye's model based on the below equation:

$$\chi(\omega) = \chi_S + \frac{\chi_T - \chi_S}{1 + (i\omega\tau)^{1-\alpha}}$$

$$\chi'(\omega) = \chi_S + (\chi_T - \chi_S)\frac{1 + (\omega\tau)^{1-\alpha}sin(\pi\alpha/2)}{1 + 2(\omega\tau)^{1-\alpha}sin\left(\frac{\pi\alpha}{2}\right) + (\omega\tau)^{2-2\alpha}}$$

$$\chi''(\omega) = (\chi_T - \chi_S)\frac{(\omega\tau)^{1-\alpha}cos(\pi\alpha/2)}{1 + 2(\omega\tau)^{1-\alpha}sin\left(\frac{\pi\alpha}{2}\right) + (\omega\tau)^{2-2\alpha}}$$

which resulted in isothermal (χ_T) and adiabatic (χ_S) susceptibilities, relaxation times (τ), and distribution parameters (α) (**Tables S2**).[4]

Table S2. Parameters of one-component Debye's model for **1**.

T / K	χ_T / (m^3 mol^{-1})	χ_T(error)	χ_S /(m^3 mol^{-1})	χ_S(error)	**α**	**α**(error)	**τ**/(s)	**τ**(error)
2.4 K	3.54E+00	6.87E-02	2.29E-01	4.42E-03	1.79E-01	6.85E-03	2.42E-03	8.74E-05
2.6 K	3.12E+00	2.65E-02	2.22E-01	3.91E-03	1.40E-01	4.67E-03	1.26E-03	1.87E-05
2.8 K	2.88E+00	1.21E-02	2.14E-01	3.52E-03	1.12E-01	3.31E-03	6.92E-04	4.93E-06
3.0 K	2.69E+00	6.53E-03	2.04E-01	3.20E-03	9.53E-02	2.51E-03	3.97E-04	1.72E-06
3.2 K	2.50E+00	3.40E-03	1.91E-01	2.59E-03	8.87E-02	1.76E-03	2.30E-04	6.38E-07
3.4 K	2.36E+00	2.52E-03	1.81E-01	2.82E-03	8.72E-02	1.68E-03	1.37E-04	3.57E-07
3.6 K	2.24E+00	2.31E-03	1.67E-01	3.81E-03	9.20E-02	1.96E-03	8.23E-05	2.63E-07
3.8 K	2.13E+00	1.62E-03	1.59E-01	4.11E-03	9.41E-02	1.79E-03	4.98E-05	1.63E-07
4.0 K	2.03E+00	1.13E-03	1.57E-01	4.62E-03	9.71E-02	1.66E-03	3.08E-05	1.15E-07
4.2 K	1.94E+00	5.87E-03	1.29E-01	4.30E-02	1.15E-01	1.18E-02	1.88E-05	6.96E-07

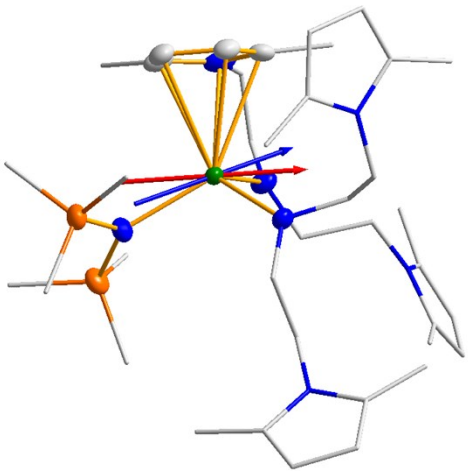

Figure S9. Direction of ground state(red) and first excited state(blue) main magnetic axes from *ab initio* calculation.

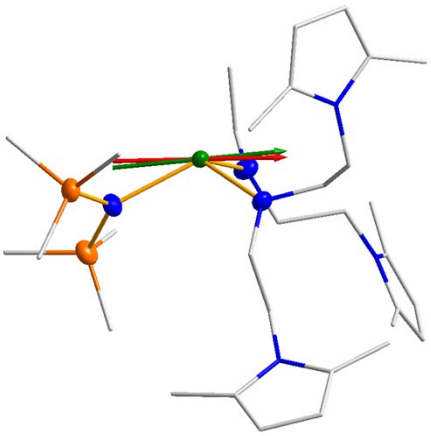

Figure S10. The reduced structure for *ab initio* calculation by remove the coordinated pyrrole ring. Red arrow and green arrow are full structure and reduced structure ground state main magnetic axis respectively.

Table S3. Low-lying spin-orbit energies, g values in three directions for full and reduced structure from *ab initio* calculation.

Kramers doublets	Full structure				Reduced structure			
	E (cm^{-1})	g_x	g_y	g_z	E (cm^{-1})	g_x	g_y	g_z
1	0	0.16	0.39	19.18	0	0.46	1.53	17.98
2	78.2	0.88	1.50	16.21	79.7	2.72	4.95	11.24
3	167.4	3.27	6.37	9.71	170.8	6.41	5.04	1.85
4	243.5	2.02	2.83	9.52	310.3	1.35	1.54	9.39
5	352.4	0.34	0.50	12.19	499.2	0.10	0.15	12.13
6	514.3	0.09	0.10	14.46	734.0	0.02	0.04	14.64
7	670.8	0.00	0.01	17.68	994.8	0.01	0.01	17.18
8	827.3	0.00	0.00	19.66	1264.6	0.00	0.00	19.74

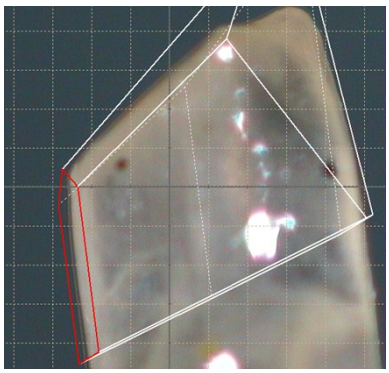

Figure S11. The picture of the crystal with size of 1.35 mm × 0.56 mm× 0.25 m

The bc-plane is defined as the XY plane. X axis is parallel to the b-axis and a*-axis is collinear with Z axis. The transformation matrix between XYZ and abc is as below.

$$\begin{pmatrix} a \\ b \\ c \end{pmatrix} = \begin{pmatrix} 0 & -0.0925 & 0 \\ 0 & 0.00226 & -0.0508 \\ 0.101 & -0.0353 & -0.00818 \end{pmatrix} \begin{pmatrix} X \\ Y \\ Z \end{pmatrix}$$

The susceptibility tensor with respect to the experimental frame is determined by simultaneously fitting the three rotation sine curves at 3 K, as depicted in Figure S10. The principle axes and the corresponding susceptibility values are therefore the eigenvectors and eigenvalues of the tensor. As shown in Figure S11(a), the $\chi_m T$ values along easy axis are large than the other two, confirming strong easy axial anisotropy. The orientation of the experimentally determined magnetization principal axes is shown in Figure 2b, where it can be seen that the axe are misoriented with respected to the crystallographic ones. Similar to diketonate supported DyIII analogues, the directions of the easy axes for the three complexes are in the plane of anti-side diketonate ligands. the experimental easy axes are consistent with the ab initio calculated axes, with deviations of 16°.

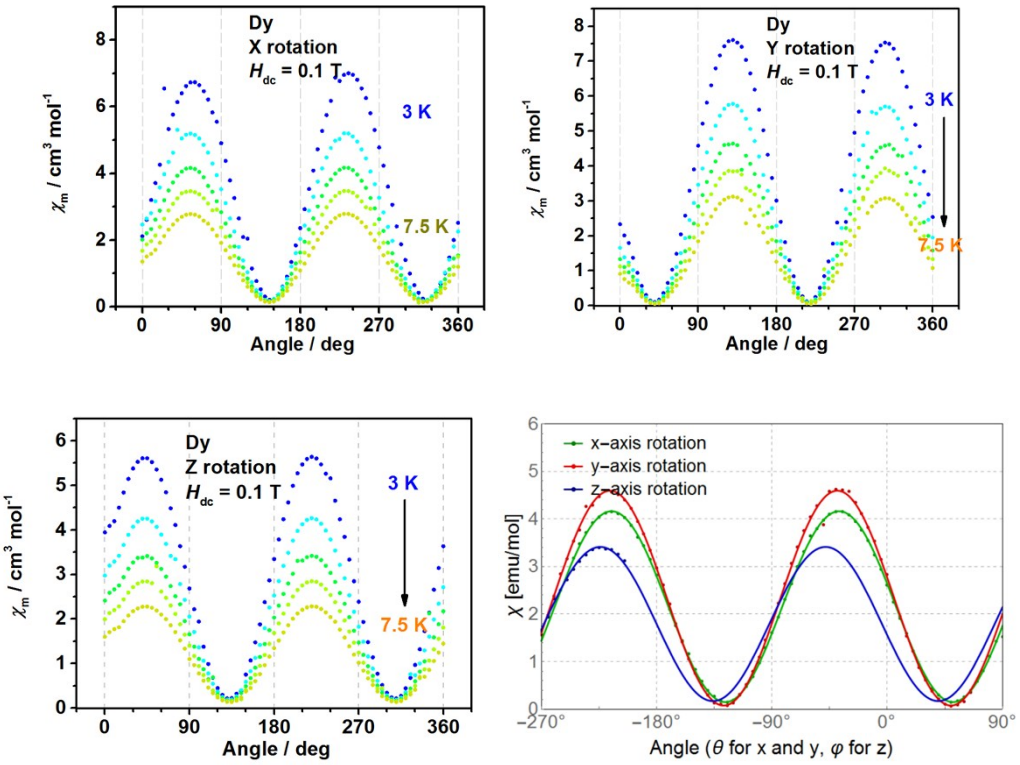

Figure S12. The magnetic susceptibility along XYZ directions from 3 K to 7.5 K (a, b, c). (d) Angular dependence of the magnetic susceptibility at 3 K under 1000 Oe dc field (circle). The red solid lines represent the best fitting result from the experimental data.

This deviation between theoretical and experimental result values can be attributed to two perspectives. In the ab initio calculations, structure deviation at different temperatures, incomplete basis and inter-molecular non-interaction assumption may all contribute to inaccurate calculations on the susceptibility values. In the magnetometry experiments, inaccurate mass and error limits of experimental measurement play an important role in the results.

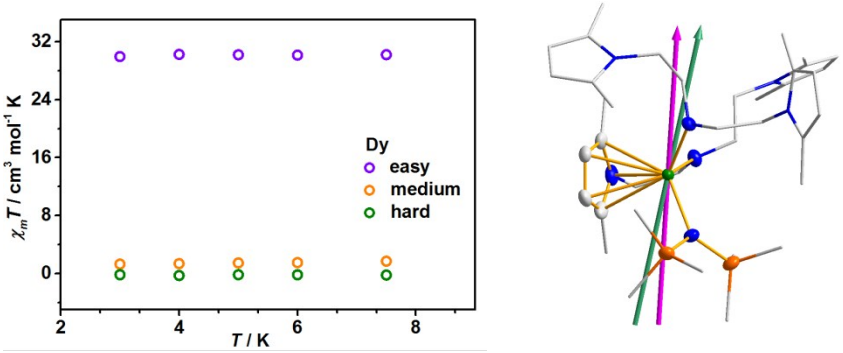

Figure S13. (a) The $\chi_m T$ values determined by angular-dependent measurements along easy (purple), medium (orange) and hard (green) axes. (b) Experimentally determined principal axes (green), *ab initio* calculation principal axe (purple).

References

1 F. H. Wang, Y. Wei, S. W. Wang, X. C. Zhu, S. L. Zhou, G. S. Yang, X. X. Gu, G. C. Zhang and X. L. Mu, *Organometallics*, 2015, **34**, 86-93.

2 G. M. Sheldrick, SHELXL-97; University of G€ottingen: G€ottingen,Germany, 1997.

3 F. Aquilante, L. De Vico, N. Ferré, G. Ghigo, P.-å. Malmqvist, P. Neogrády, T. B. Pedersen, M. Pitoňák, M. Reiher, B. O. Roos, L. Serrano-Andrés, M. Urban, V. Veryazov and R. Lindh, *J. Comput. Chem*., 2010, **31**, 224.

4 D. Gatteschi, R. Sessoli and J. Villain, *Molecular Nanomagnets*, Oxford University Press, Oxford, 2006.

5 S. D. Jiang, B. W. Wang and S. Gao, *Molecular Nanomagnets and Related Phenomena*, Springer Berlin Heidelberg, 2015.